

Master's thesis

2019

Master's thesis

Kaja Sofie Lamvik

NTNU
Norwegian University of
Science and Technology
Faculty of Engineering
Department of Mechanical and Industrial Engineering

Kaja Sofie Lamvik

Monitoring of Composite Repair on Risers

June 2019



Norwegian University of
Science and Technology

Monitoring of Composite Repair on Risers

Kaja Sofie Lamvik

Materials Science and Engineering

Submission date: June 2019

Supervisor: Nils Petter Vedvik

Norwegian University of Science and Technology
Department of Mechanical and Industrial Engineering

PREFACE

This report was written during the spring semester of 2019 as a finalization to the master program Materials Technology at NTNU, with the specialization of Materials Development and Use.

Prior to the execution of the master project, a preliminary study that resulted in a project report was carried out. Giving theoretical background and valuable practical experience, the findings of the project report was to a large extent included in this thesis.

The work was written in collaboration with Kongsberg Ferrotech, with the aim of the final report to present a suitable monitoring technique for their needs, with its potential demonstrated.

I would like to thank my supervisor, Nils Petter Vedvik, for great guidance throughout the duration of the project. Further, thank you to Brede Thorkildsen and the contacts at Kongsberg Ferrotech for the good cooperation. Thank you to Eivind Hugaas and Erik Sæter for guidance and tips with the practical use of the OBR and optical fibers, and to Carl Magnus Midtbø and Børge Holen for assistance in the workshop. Finally, thank you to my father, Trond Lamvik, for the moral support and insightful suggestions.

ABSTRACT

The presented study is completed in cooperation with Kongsberg Ferrotech, whom is developing an autonomous robot to perform composite repair on offshore risers. By developing such an effective repair process, composite repairs have the potential of becoming more conventional.

The aim of this project was to find an effective method to monitor the quality and integrity of composite repairs. It was clear from the preliminary study [1] that the optical backscatter reflectometer (OBR) was the most promising monitoring technique to utilize in strain monitoring of composite repairs on risers, which gives high resolution measurements and large measurement range using optical fibers.

The OBR's capabilities were investigated through thermal cycling tests in water. Moreover, a test sample consisting of a pipe section, embedded optical fibers, a glass fiber composite repair including predefined failures were subjected to temperature variations over a certain period of time. Finite element analysis (FEA) was performed to support the findings of the experiments.

The results confirmed that OBR monitoring is suitable for the given application, and successfully showed signs of damage at an early stage. No growth of detected failures was recorded, which indicates that the repair possessed satisfactory qualities. Both predefined failures and other possible failures were found, however variations in strain response may be caused by factors not associated with failures in the glass fiber composite or the substrate.

SAMMENDRAG

Denne studien var utført i samarbeid med Kongsberg Ferrotech, som utvikler en autonom robot som skal utføre komposittreparasjoner på offshore stigerør. Ved å utvikle en slik effektiv reparasjonsprosess har komposittreparasjoner potensialet til å bli mer konvensjonelt.

Målet med prosjektet var å finne en effektiv metode å overvåke kvaliteten og integriteten til komposittreparasjoner. Fra forstudien [1] var det tydelig at et optical backscatter reflectometer (OBR) var den mest lovende overvåkningsteknikken, og er en overvåkningsteknikk som gir målinger med høy oppløsning over et stort måleområde ved å bruke optiske fibre.

Egenskapene til OBRen ble undersøkt i termisk sykling tester i vann. En rørseksjon, innstøpte optiske fibre, en glassfiberreparasjon med innstøpte feil utgjorde testprøven, og ble utsatt for temperaturendringer over en viss tid. De eksperimentelle funnene ga en tydelig indikasjon på debonding hvor de innstøpte feilene var, og elementanalyse (FEA) var utført for å støtte funnene.

Resultatene bekreftet at OBR overvåkning er egnet for denne applikasjonen, og viste tegn på skade på et tidlig stadium. Ingen vekst av detekterte feil ble registrert, noe som indikerer at reparasjonen hadde akseptable egenskaper. Både forhåndsdefinerte feil og andre mulige feil ble funnet, men variasjoner i tøyingsrespons kan være forårsaket av faktorer som ikke er forbundet med feil i glassfiberkompositten eller substratet.

CONTENT

Preface	I
Abstract	III
Sammendrag	V
List of Figures	VIII
List of Tables	IX
1. Introduction	1
1.1 Project description	1
1.2 Project scope	1
1.2.1 Limitations	1
1.2.2 Research questions	2
1.3 Thesis structure	2
2. Background	3
2.1 Corrosion of offshore pipelines	3
2.1.1 Corrosion	3
2.2 Conventional repair systems	4
2.3 Composite repair systems	4
2.4 Challenges with composite repair	5
2.5 The presented application	6
3. Theory	9
3.1 Qualification	9
3.1.1 Overview	9
3.2 Monitoring and monitoring techniques	10
3.2.1 Requirements for a monitoring system	11
3.2.2 Optical Backscatter Reflectometer	11
4. Case study configuration	17
4.1 Estimate of expectations	17
5. Tests	19
5.1 Objective	19
5.2 System requirements	19
5.3 Preparation of the optical fiber	20
5.4 Experimental plan	20
5.4.1 Test procedure	20

5.5	Execution	23
6.	Finite Element Analysis	25
6.1	Model.....	25
7.	Results and discussion.....	29
7.1	Strain in relation to temperature	30
7.2	Debonding	31
7.3	Strain data from test and FEA	33
7.4	Visual inspection	34
7.5	Noise.....	34
7.6	Evaluating quality of results	35
7.7	Conclusion.....	37
8.	Conclusion.....	39
9.	Further work.....	41
10.	References	43

LIST OF FIGURES

Figure 1 – A repair (light gray) applied on a riser (dark gray) in the splash zone.	17
Figure 2 – Primary and secondary optical fiber spliced.....	20
Figure 3 – Equipment used for the preparation of optical fibers.	20
Figure 4 – A: Configuration of optical fibers and Teflon films. B: Turns were kept smooth. C: Four pieces of Teflon film. Two different sizes were used.....	21
Figure 5 – The test sample assembled in the filament winding machine.....	22
Figure 6 – The glass fiber composite patch protected the optical fibers. The repair possessed good quality. These images were taken after the testing.....	22
Figure 7 – A: Schematic of the test setup. B: Test setup.	23
Figure 8 – Model of riser and repair.	26
Figure 9 – A: Two boundary conditions were defined. B: Mesh of the model.....	26
Figure 10 – Strain distribution for the top surface (left) and bottom surface (right).	28
Figure 11 – Configuration of optical fibers and location of reference points.	29
Figure 12 – Temperature cycles. The area marked in red was not considered part of the main test execution and was in some cases disregarded.	30

Figure 13 – A, C and D: Heating cycles gathered from measurement 66 (blue) and 125 (red). B: Temperature cycles throughout the test duration. Measurement 66 and 125 are marked with a blue and red dot respectively.	30
Figure 14 – There was an obvious lag between temperature and strain.....	31
Figure 15 – The debonding characteristic changes according to the temperature.	31
Figure 16 – Development of the debonding failures detected by OF3 and OF4.	32
Figure 17 – Development of a new failure.....	32
Figure 18 – Appearance of the repair after the execution of the test.	34
Figure 19 – Strain curves from measurement 5. The strain curve on the left is shorter because a different mid-point was used for the calculation.....	35
Figure 20 – Strain curve from measurement 5 without noise.	35

LIST OF TABLES

Table 1 A, B – Properties of the numerical model.....	25
Table 2 – Strain values obtained from FEA corresponding to the positions of the optical fibers. The notation a and b correspond to the first and second circumferential placement of the optical fiber respectively.	27
Table 3 – Reference points and their corresponding location on the optical fiber.....	29
Table 4 – Strain from FEA and measurement.....	33
Table 5 – Strain from FEA and measurement.....	33

1. INTRODUCTION

1.1 PROJECT DESCRIPTION

A riser is a vertical pipeline transporting petroleum products from subsea installation to topside installation. The riser operates in harsh environments, moreover the external surface is exposed to degradation mechanisms such as seawater corrosion, which is a life limiting condition. The riser is originally protected against corrosion by e.g. a rubber coating in the splash zone, but in severe cases of external corrosion the riser may be repaired to restore its maximum functionality and production capabilities, furthermore, to extend its lifetime. Composite materials are promising materials to utilize in repairs; wrapping the riser in such materials gives the potential of a time and cost-effective repair process and a final repair with suitable strength. The initial damage is restored, but problems may still arise when it comes to the repair system itself as failure mechanisms like debonding and delamination can occur. Thus, monitoring the behavior of the repair can verify that the quality of the repair is sufficient and structural integrity is intact.

Failure can be detected and disasters prevented by proper monitoring of the repair system. Here, a suitable monitoring technique is elaborated on and put to test in lab experiments and finite element analysis.

A preliminary study was conducted prior to the execution of this thesis, where different monitoring techniques were evaluated, and the most promising technique was further investigated. Its potential was demonstrated with the aid of simple tests. The preliminary study was finalized in a project report [1], which provided theoretical basis for this report as well as practical experience and potential for improvement on the experimental tests. The background and theory presented in this report is to a large extent the same as what was presented in the project report.

1.2 PROJECT SCOPE

The main objective of the complete work, included in a project report and a master thesis, is investigation, development and testing of methods for monitoring the quality and long-term integrity of composite repair on risers. The project report includes a literature review on common monitoring techniques, where the most promising one was investigated further by conducting a simple test as well as finite element analysis. This master thesis builds on the discoveries made and the experiences gained from the project report to further investigate the implementation of the optical backscatter reflectometer (OBR) and optical fibers in the given application of composite repairs on risers. Here, more thorough tests in addition to more accurate finite element analysis are presented.

1.2.1 LIMITATIONS

If the discoveries are to be considered for implementation out in the field, it may be included in an autonomous repair process. The evaluation of monitoring techniques considers how the

device may be included in the structure, i.e. embedded or not, but does not consider the application process onto the riser offshore.

The optical fiber's response to thermal loads are studied, rather than mechanical loads. The temperature effects that occur in the optical fiber itself when subjected to such loads over a long period is disregarded. These variations can to some extent affect the measurements, and it is therefore recommended to further investigate this phenomenon if implemented out in the field.

The monitoring is limited to the behavior of the glass fiber composite repair, and not the initial damage. It is assumed that the initial damage is fully restored by the repair.

1.2.2 RESEARCH QUESTIONS

A promising method of interpreting the behavior of the repair was investigated, furthermore the relative deformations that occurred inside the repair when subjected to appropriate loads was studied. How can one ensure that the quality of the performed repair system is satisfactory?

1.3 THESIS STRUCTURE

The thesis is introduced in Chapter 1, where the project, scope and limitations are described. In Chapter 2, the background for the project is presented, where riser repairs are elaborated on and the failure modes associated with composite repairs are examined. The field of application is clarified. Chapter 3 begins by giving an overview of qualification and briefly examines relevant standards. Further, a review of relevant research is presented to acquire theoretical basis and experience to establish a solid foundation for the monitoring technique chosen. The monitoring technique is evaluated by experimental tests in Chapter 4, including preparation and production of test sample as well as test execution. In Chapter 5, the numerical analysis is described. The results are presented and discussed in Chapter 6, moving on to final conclusions and further work in Chapter 7 and 8 respectively.

2. BACKGROUND

The preliminary study conducted prior to this resulted in a project report. The background presented in the project report is highly relevant to this thesis and is therefore included here. For further information on the project report, see [1].

2.1 CORROSION OF OFFSHORE PIPELINES

An oil production riser is the pipeline that transports petroleum products from seabed to topside. This component operates in the splash zone, which is defined as where an external surface is periodically in and out of water [2], and is affected by the influence of waves, tides, vertical motions etc. The oxygen and water supply of the splash zone creates a very corrosive environment. [3] Sacrificial anodes is an effective method to protect equipment and structures against corrosion subsea, but as there are no stable electrolytes around the component in the splash zone this is not an alternative [4]. Therefore, the riser is rather protected by other means, like rubber coatings [5]. Corrosion is one of the main failure modes in offshore structures and equipment and is responsible for 40 % of reported riser incidents [6]. This emphasizes the importance of protection to prevent corrosion like surface treatment, as well as repairs when the corrosion is severe.

The riser's exposure to failure can be described as the typical bathtub pattern, where the riser is more prone to damage early on and late in its lifetime because of inherent defects and time related failure mechanisms respectively [7]. Inspection and maintenance can reduce the occurrences of such failures, furthermore risers are repaired to restore the component to a functional level and to extend its lifetime. Thus, time related failures are put off [7].

2.1.1 CORROSION

40 % of reported riser incidents are caused by corrosion [6] and is one of the main failure modes in offshore structures. This emphasizes the importance of protection to prevent corrosion like surface treatment, as well as repairs when the corrosion is severe.

Corrosion is defined as “the deterioration of a substance - usually a metal - or its properties because of reaction with its environment.” [8] There are three main components that are necessary for corrosion to occur; a material (usually a metal), oxygen and an electrolyte, e.g. water. [9] To deteriorate the material by corrosion, one anodic and one cathodic reaction occur separately, that is to disperse and absorb electrons, respectively.

The main corrosion types to occur on a component like the riser are uniform, crevice or pitting corrosion.

UNIFORM CORROSION

This is a type of corrosion that evenly distributed over the metal surface, provides a predictable corrosion rate and gives an even reduction in thickness. For this to occur, the electro chemical corrosion must be the only attack on the material, and the chemical reactions must act on the entire surface. Additionally, the metal and the distribution of ions must be relatively homogeneous. [10]

When the structure deviates from the requirements for the uniform corrosion, other types of corrosion are induced. The deviations can be environmental forces and surface conditions like roughness. [10]

CREVICE CORROSION

Corrosion may also be concentrated in smaller areas. If a crevice is formed, e.g. underneath bolts and nuts, lap joints and coatings and especially where the coating is damaged, it will accumulate water [10]. If the crevice is small enough, the oxygen will dissipate away from the initial corrosion. Consequently, the crevice is anodic and the corrosion speed in the crevice will increase.

PITTING CORROSION

Similar to crevice corrosion, pitting corrosion attacks small, concentrated areas. Pitting may initially be caused by surface irregularities like scratches [11] and because of exposed metal due to broken coating [12]. This localized change in geometry of the metal allows for changes in the water chemistry. The corrosion speed in the pit will increase because of the chemical corrosion reactions will create a more and more corrosive environment in the pit. [10] Pitting corrosion is uncontrollable and is usually avoided by choice of materials as some are more prone to pitting corrosion than others.

2.2 CONVENTIONAL REPAIR SYSTEMS

There are several conventional repair systems used to repair corroded pipelines and risers. Removing the pipe completely or replacing parts of it is of the most common methods. Furthermore, one can install a steel clamp or sleeve around the corroded section, which are either bolted or welded in place. All these methods provide enough strength to the riser for it to function as if no damage was done, but the installment of such repair systems is difficult. Heavy machinery is needed, and welding poses a risk of fire and explosions. These repair methods are mainly suited for straight sections of the riser or pipeline. In conclusion, these repair systems are expensive, time consuming and inflexible [13].

2.3 COMPOSITE REPAIR SYSTEMS

Composite repair techniques are established in several applications in other industries. In airplanes patches of composites are applied to slow down crack growth or repair corrosion [14],

similarly this technique has been used to repair corrosion defects and cracks in metal structures on ships [15] as well as repairing and reinforcing bridges [16].

The challenges with the conventional repair techniques gave the desire for a new approach for pipeline and riser repair. Technologies for utilizing composites in riser repair was developed in the late 1980s. Composite repairs are advantageous to the conventional repair techniques because of its designability and a production method that does not require welding, as well as being more cost-effective. The composite repair is on average 24 % cheaper than the repair technique of welding the steel sleeve [13]. Additionally, it is a safer and simpler repair technique, and does not require a shutdown period.

There is a wide range of design possibilities of composite repairs, but will usually consist of a fiber reinforcement material, like glass or carbon fiber composite, adhesive material and defect filling. The respective materials are of high strength, and the composite can be of the type pre-cured layered, preimpregnated, flexible wet lay-up, split composite sleeve or a flexible tape system. The composite material is wrapped around the defected section of the riser and can restore damages of up to 80% loss of material. [13]

2.4 CHALLENGES WITH COMPOSITE REPAIR

Although the composite repair is a promising repair technique, it is not commonly used as a permanent repair method because of the uncertainties related to its long-term performance. The respective materials of the riser and repair have differences regarding coefficient of expansion, elastic modulus etc. Consequently, the repair can undergo failure mechanisms when the riser is subjected to temperature changes and external environmental forces as well as the internal operating pressure of the riser. The failure modes of the repair are mainly patch debonding, patch failure and substrate failure.

PATCH DEBONDING

Debonding refers to the lack of cohesion between the glass fiber composite and substrate. The riser and repair do no longer have a uniform connection, and the repair system is left weakened. If such a failure mode occurs, the riser can corrode underneath the repair, which can lead to further debonding [17]. Debonding may affect the material properties of the glass fiber composite. Cracks can be initiated on the bondline if the loads transferred through the repair exceeds the allowable loads that the bondline can stand. These initiated cracks can propagate to fracture. Similarly fatigue cracks may be initiated and propagated in the case of repeated load cycles, resulting in debonding. Debonding can also be caused by creep rupture, where the creep will affect the cohesion between repair and riser. [18]

REPAIR FAILURE

If the strain in the repair exceeds a critical level, cracks can start to form in the matrix and the repair will fail due to matrix cracking. Moreover, if the repair is subjected to loads exceeding

its capacity, cracks can be initiated and propagated to give fractures. Consequently, the repair is left weakened and will not be able to carry the necessary load. [18]

SUBSTRATE FAILURE

If the added strength of the repair is not sufficient, the damages in the substrate may proceed. The damages may have been so severe that the thickness reduction of the riser is too large, consequently the repair will not provide the required strength. [18]

CONCLUSION

The integrity of the repair is significantly dependent on the production quality, which generally can be optimized by thorough lab testing and good practices during production. To limit the occurrences of the respective failure modes, or to discover the occurrence at an early stage and hence restrict the subsequent damage, a way to monitor the behavior of the repair is needed. Moreover, non-destructive verification of the repair is vital when incorporating a life-extending feature such as a glass fiber composite repair. [17]

2.5 THE PRESENTED APPLICATION

Kongsberg Ferrotech is a subsea robotics company that develops an autonomous robot to perform such composite repairs on risers. It is designed to carry out the process of inspection, repair and maintenance in a cost-effective way, moreover the autonomy discards the need of ROVs or divers. This solution is advantageous to others because there are reduced HSE risks and no shut-down time. [19]

The effective repair process consists of two stages where the robot is equipped with different modules. First, it is equipped with the surface repair module; the chamber of the robot closes around the damaged area and creates a stable environment by flushing the water out. The surface preparation consists of obtaining a surface clean from salt, corrosion, old coating etc. by using a grinder. A corrosion resistive coating is applied giving a thickness of 500 μm and 50 mm overlap with the old coating. The surface preparation is complete, and the chamber is filled with seawater. The equipment is changed to a structural repair module. A stable environment is again obtained by emptying the water and cleaning the surface. The repair is applied using Syntho-Glass XT Pipeline Integrity Kits, which consists of epoxy filler, sealant system and glass fiber composite. A compressive film is usually utilized in this kit, but here the glass fiber composite is applied with tension, which evades the need of the compressive film. Tension ensures consolidation between the layers. The glass fiber composite is bi-directional and has a polyurethane matrix, moreover the curing process is induced by spraying water upon application. The repair is complete.

The method is limited to repair a reduction of wall thickness up to 80 %. The repair process is intended for offshore operations in Malaysia. Risers having been operating for 50 years is not uncommon, and although protected from corrosion by coatings and rubber covers, the external

corrosion attacks of these risers are severe. The application of the repair is intended for life-extension.

3. THEORY

3.1 QUALIFICATION

Qualification of a component documents that the structural integrity of the component is preserved. Monitoring of components is a central part of the qualification process.

3.1.1 OVERVIEW

To be a qualified structure, theoretical assessments and verification by testing is performed with the guidelines of relevant standards. Moreover, the design, installation and maintenance that applies for the specific application must be within the requirements of standards or else it cannot be in service. Following, the most relevant standards are presented, and its qualification process is briefly explained.

DNV-GL OS C501: COMPOSITE COMPONENTS

This standard applies to any application where composites are used and gives requirements and recommendation for design and analysis of composite components, including modification, operation and upgrading these components. Environmental loads and conditions related to the offshore industry are emphasized, and gives aspects on documentation, verification, inspection etc. Requirements for composite repairs are given, which are based on achieving the same level of strength and functionality as the original structure. A composite repair is essentially a laminated joint, where the most critical component is the interface for load transfer.

Testing can be carried out to qualify the component or to verify analysis or design calculations. Testing and analysis shall show that no failure will be critical for the functionality and safety of the component. For the given application, where long-term performance is to be demonstrated, the evaluation of possible failure mechanisms is essential.

The test specimens must be representative of the actual component. The test results are only valid for the load cases and the environmental conditions tested. Failure mode(s), failure mechanism(s) and location(s) of failure must be recorded and verified.

When exposed to environmental conditions over a long period, i.e. a year and longer, the physical properties of the composite are affected, and the effects usually increase with time. The fiber and matrix respond to the environmental conditions differently due to their difference in chemical nature. The fiber matrix interface, as well as void content and matrix cracks, influence the environmental resistance.

The environmental conditions considered in the standard are temperature, water, chemicals and UV radiation. Seawater is considered to give a less severe effect than fresh water. The combination of water and high temperature influence the composite more severely than if the influence occurred individually.

ASME PCC-2-2015: REPAIR OF PRESSURE EQUIPMENT AND PIPING

This standard explains how to design, fabricate, examine and test repairs of equipment and pipes during their service life. This standard is mainly applicable for general applications and may not be appropriate for all applications.

Mechanical and thermal properties, like tensile strength, in-plane shear modulus, lap shear adhesion strength and thermal expansion must be determined by testing. A minimum value (if applicable) is stated and which test method that applies for which property is stated.

DNV-RP-C301: DESIGN, FABRICATION, OPERATION AND QUALIFICATION OF BONDED REPAIR OF STEEL STRUCTURES

This document provides guidelines and accepted practices for bonded repairs. Such repairs are sensitive to environmental loads, and its degradation may be accelerated because of chemicals and thermal loads. Non-destructive inspection methods such as ultrasound and x-ray are suggested to detect delamination in the laminate, but no technology is suggested for detection of damages in the bondline.

Long term tests are necessary to document the effects of thermal loadings, if the repair is to be exposed to thermal fatigue.

DNV-RP-A203: QUALIFICATION OF NEW TECHNOLOGY

This recommended practice gives a systematic approach to qualifying new components, equipment and assemblies that utilizes new technology, mainly for offshore applications. Moreover, qualified technology in a new setting or already qualified components assembled in a novel fashion is considered a new technology.

The qualification process is based on five steps. First, the qualification basis is elaborated on and the qualification requirements are set. Further the technology is assessed where challenges and uncertainties are identified. The threats are evaluated, and the failure modes are recognized, with their level of criticality determined by risk to the component and overall system. Further the activities required for the qualification is planned, and finally executed and documented.

3.2 MONITORING AND MONITORING TECHNIQUES

Proper monitoring is necessary to ensure that the repair provides the strength and functionality as if no damage was present. The long-term performance of bonded repairs is uncertain, and one purpose of bonded repair is to prevent damages from becoming critical. Defects such as debonding and delamination can be detected by monitoring, which are both failures that compromise the efficiency of the repair [18]. Applying the repair, and thus repairing the damage, poses a problem of inspecting the original damage. The damage is no longer visible, and a new approach for inspecting and monitoring the damage is needed. [20] Selecting a suitable monitoring technique is required to upholding credible measurements.

3.2.1 REQUIREMENTS FOR A MONITORING SYSTEM

There are several requirements for the monitoring technique to be successfully implemented in the given application. First, it must examine a parameter that can detect the relevant failure modes. Strain is one of the most central parameters when it comes to detecting mechanical failure such as the given failure modes, because if any of those occur, changes in strain will be present. Furthermore, the strain response in a composite material will not be uniform. [21] Therefore, the monitoring should have a suitable spatial range to relate the measurements to the entire repair rather than one single point.

The sensor implemented into the repair must be non-destructive and not introduce damage to the system, like weak spots, crack initiators or sharp corners. The repair and the monitoring device are to be implemented in a risky environment sensitive to electrical sparks. Elements introducing fire hazards must be avoided.

It is important to keep in mind that the part most relevant to monitor is the interface between the pipeline and the repair. This is where debonding is most likely to occur, and defects occurring in this interface are more critical than those occurring in the interface between plies as it is the only load path [22]. Therefore, the sensing device should be implemented on this interface.

Several monitoring techniques were evaluated in the preliminary study [1], and the above-mentioned factors were considered when deciding on a suitable monitoring technique. Implementation possibilities were divided into embedded or surface mounted.

It was clear that using the optical backscatter reflectometer (OBR) was the optimal monitoring technique to utilize. The OBR utilizes optical fibers as sensors, which can be applied around the riser in different directions, moreover it gives a larger measurement range than the alternatives. The optical fibers can be embedded in the repair to monitor the position of interest, without significantly influencing the repair. The measurements are independent of the surrounding conditions.

3.2.2 OPTICAL BACKSCATTER REFLECTOMETER

Fiber Optic Sensors (FOS) is the common term for the sensors that interpret and analyze the reflections of light in optical fibers. Distributed FOS (DFOS) develop temperature or strain fields based on the scattering process that occurs in the optical fiber, which is interpreted by the software. [23] The optical fiber has a small diameter of 155 – 195 μm [24], a very high spatial resolution and is sensitive enough to detect small changes, while still providing a large measurement range. The measurement range can be very long and can vary from one to several thousand meters, but the length will compromise the spatial resolution of the measurements. The spatial resolution is the accuracy at which the data is acquired and can be down to ~ 1 mm. [23]

The optical backscatter reflectometer (OBR) is an instrument that is used to detect changes in strain using optical fibers. The software enables continuous measurements along the entire length of the optical fiber. The optical fiber is carefully placed over the areas that are to be studied, which is referred to as primary fibers, and connected to the OBR via protected optical fibers, referred to as secondary fibers. The optical fiber is often embedded in composites or polymers, but it can easily break when composite production equipment is removed. The optical fiber is usually placed along the composite fiber direction. [25]

The OBR emits a laser beam from the light source, giving a probe signal. The natural imperfections or the varying reflective index over the length of the optical fiber cause Rayleigh backscattering. This backscattering is the detected signal, where information from the reflected pattern and the backscatter time gives continuous sensing points along the optical fiber. This reflection pattern will change when the optical fiber deforms. [25] The signal can be compared to a reference signal and converted into a function of length. The strain response will comply to the entire length of the optical fiber in one measurement and give information about the overall behavior of the structure. [24] The optical fibers can be arranged in a grid to provide two-dimensional strain fields. [25]

Parameters such as gauge length and sensor spacing are defined in the software, which describe the virtual sensors along the optical fiber's length. Strain is found by averaging the displacement of the backscattered signal over the gauge length, which is done for each virtual sensor [25]. When the gauge length is larger than the sensor spacing, the measurement points will overlap. The number of measurement points is given by the sensing length divided by the sensor spacing. These parameters are set by the user and the optimal combination is different for each measurement, as measurements with a short gauge length will contain more details while a long gauge length reduce scatter in the measurements.

Using the OBR for strain measurements is a relatively new technology but is proven to be a promising measurement technique in several publications [26 – 33]. The practical implementation of optical fibers is often time consuming and cumbersome, so gaining experience from other researchers can be beneficial. Following is a review on research results from the open literature [26 – 33].

In Grave et al. [26] the OBR was used to measure the strain field developing in a composite patch adhered to a metal I-beam when a four point bending test was performed. At the center of the top flange of the I-beam there was machined crack of 20 mm terminated by a 6 mm hole. The composite patch was of carbon fiber composite with a coating of chopped strand mat underneath, that worked as a galvanic protection layer. The optical fiber was placed in two locations; one was embedded in the composite laminate and would measure the strain originating from the adhesive interface while another optical fiber was placed on the surface of the composite patch. Additionally, four electrical strain gauges was placed on the patch surface for comparison. A numerical model was made in Abaqus 6.11-1, where tie constraints were made between the three parts, the parts shared nodes and the parts were sectioned in the same places. There was a clear agreement between the respective strain measurements at low

loadings, revealing a strain field peaking at the location of the crack. At high loads, the strain field possessed the same shape as for low load levels but were elevated. However, the strain obtained at high loads from the physical test differed from what was obtained from the linear finite element analysis. The reason for this was damage development in the composite, which was not included in FEA, but proves the OBRs potential of detecting damage at an early stage. High strain gradients gave noise in the measurements but was improved by postprocessing. In conclusion, the OBR was successfully used to evaluate the repair.

Optical fibers can be embedded in the composite material, which is successfully performed in the work carried out by Sæter et al. [27]. The objective was to validate the use of the OBR as a structural health monitoring method for composite pressure vessels. Impact and burst testing were performed to investigate this method for structural health monitoring. The configuration of optical fibers gave high-resolution strain measurements from the entire pressure vessels' surface. The optical fibers are usually placed parallel to the composite layup, but for filament wound structures this will not be precise. The optical fibers were embedded between hoop layers, but the optical fibers and composite layup had different pitch angles. The optical fibers were placed with a 20 – 30 mm spacing which gave a pitch angle of 2.6° – 3.9° , while a pitch angle of 0.65° was used for the composite fibers. This offset gives resin-rich areas around the optical fibers in addition to voids, and if the composite material undergoes matrix cracking due to high load levels, the matrix cracks can induce high local strains around the optical fiber and disrupt the signal. However, the difference in pitch angle is relatively small and will only cause minor disturbances to the laminate, and the properties of the composite are not expected to be notably affected. Optical fibers were also applied in a grid located on the center of the pressure vessel, which would measure strain from impact loads.

Several fibers failed at the point where the fiber egressed from the laminate when disassembling from the filament winding machine; only 50 % of the optical fibers were intact after production. By applying a patch of glass fiber composite over the area where the optical fibers were vulnerable, this problem was solved and almost all fibers remained intact.

The strain measurements were performed using the OBR 4600 delivered by LUNA. The resolution can be altered by changing the settings for sensor spacing and gauge length. Essentially, the gauge length is the length of a virtual strain gauge while the sensor spacing is the spacing between these strain gauges. Differently from regular strain gauges, these virtual strain gauges can overlap. In the experiments performed in Sæter et al. [27], three different set of parameters were utilized; gauge length of 5, 10 and 30 mm and a sensor spacing of 1, 5 and 10 mm respectively. Using a gauge length of 5 mm and a sensor spacing 1 mm will give very fine spatial resolution but may also introduce local fluctuations in the measurements. If the strain field is close to uniform and a high spatial resolution is not needed, these fluctuations can be averaged and therefore avoided using a coarser resolution.

Measurements containing noise is a common occurrence. The strain measurements discovered in Sæter et al. [27] suffered from noise as the load levels got higher. Faulty splices, bad connections or excessive curvature in the secondary or primary coated optical fiber can often

be reasons for added noise. Damages around the optical fiber can also result in a signal containing disturbances; this includes both impacts or possible voids around the optical fiber. As previously mentioned, voids and resin rich areas are common when the orientation of optical fiber and composite fiber differ, hence a larger pitch offset yields higher noise levels. Post processing can also give noise; some settings for strain calculation can introduce more noise.

The experiments performed in Sæter et al. [27] was also the basis for another report, Lasn et al. [28], where one of the main objectives was to locate the damage detected by the OBR. When studying damage caused by impact, the simplest detection approach only relies on the optical fibers backscattered signal. The end of the optical fiber is seen in the measurements as a high peak. If the optical fiber breaks due to a high load, the end, and hence the peak in the measurements, will change its location. Although this approach is very simple and effective, it is only useful if the fiber breaks. This will also entail that less data can be acquired in any further measurements.

In Lasn et al. [28], strains were calculated in a network of optical fibers when subjected to an impact load. To localize the damage a strain map was constructed in post-processing, where a value of strain was represented by a dot and its location was given by hoop and axial position. A larger value of strain was represented by a larger dot. This did not only localize the damage, but also visualized the shape of the damage. The orientation of the damage aligned with the helical orientation of the composite fibers, which were wound at $\pm 15^\circ$ to the axial direction.

In the analyses performed by Heinze et al. [29] as well as Sæter et al. [27], strain was determined by a running reference method rather than comparing each measurement to an initial reference. The running reference method determines strain by comparing each measurement to the previous measurement, and an absolute value of strain is found by adding all the strain differences. When the optical fiber is under certain physical conditions, e.g. micro bending or pinching, noise will be introduced to the measurements and the obtained strain values will not necessarily be meaningful. The running reference method, however, determines meaningful strain measurements with reduced noise in circumstances where the traditional method fails, e.g. previously mentioned conditions for the optical fiber or very high load levels [27]. Nevertheless, noise will be present at very high load levels (close to failure) and around damaged areas but can be interpreted as a sign of damage like matrix cracks.

Composite materials subjected to impact loads are vulnerable to undergo delamination, especially in the vicinity of free edges. Díaz-Maroto et al. [30] used the OBR to detect and localize delamination. Optical fibers were placed in a dense network with 5 mm spacing between each fiber, both embedded and attached to the surface. As a response to delamination, the optical fiber attached on the surface will undergo residual strains, which will indicate the location and extent of damage. Experimental tests were conducted to detect delamination on composite laminate plates with a $[0_n/90_n]_S$ layup, where the number of layers n were 2 or 4 for different specimens. The specimens were subjected to impact loads by a drop-weight testing machine. Delamination was found both on-edge and near-edge. In the first case delamination was detected and verified by visual inspection. In the latter case, the damage was internal and

could not be detected by visual inspection but was verified by ultrasonic C-scan inspection. The measurements recorded a delaminated region with $200 \mu\epsilon$ change in the residual strain field. In conclusion, the OBR was a suitable technology to utilize for the detection and localization of delamination in composites.

Optical fibers are commonly utilized for the monitoring of composite bonded lap joints, which is an effective joining method for composite structures. It has been proven to be a promising way of monitoring such structures by Bernasconi et al. [31] and Wong et al. [32], both of which performed fatigue tests. The former subjected a single lap adhesively bonded CFRP joint to a 3,5 kN load with a test frequency of 10 Hz until failure at $\sim 60\,000$ cycles. The optical fiber was configured with bends to monitor four segments on the front surface and two segments on the back surface using one single optical fiber. The measurements were obtained every 5000 cycles at the mean load value by pausing the test. The full strain profile was obtained from the OBR measurements, and a minimum strain value as recorded. FE analyses were performed. A linear correlation between minimum strain and crack length was found.

Wong et al. [32] performed a fatigue test on a flush step lap joint of CFRP. One optical fiber was bonded to the surface in a loop, monitoring the joint along its two edges. An extensometer correlated strain to load. The specimen was subjected to a peak strain of $1000 \mu\epsilon$ with a frequency of 5 Hz and increased to $2000 \mu\epsilon$ after $100\,000$ cycles. The test was running until failure which occurred at $\sim 250\,000$ cycles. The measurements clearly indicated damage before the failure occurred as increased strain values in the last 3500 cycles. Wong et al. [32] concluded that the optical fiber sensors proved to be a promising technique for damage assessment and monitoring of fatigue crack growth which has promising possibilities for implementation in structures for monitoring while in use.

Previously mentioned research is mainly focused on lab-experiments. In a study by Barrias et al. [33] the OBR was implemented for monitoring real structures in Barcelona. The Sarajevo Bridge in Barcelona, Spain, was monitored while undergoing construction without closing the bridge for traffic. The objective was to detect changes in the structural behavior of the bridge as well as determining the bridge's structural safety during and after construction. Optical fibers were placed along the length of the bridge in areas prone to stress increments and cracking. Readings were performed on two optical fibers of 50 m. The monitoring lasted for a time period of 9 months, where the readings were obtained in certain monitoring periods. Over such a long monitoring period, the temperature variations do not only affect the behavior of the structure but also the optical fiber. Both the refractive index and the material of the optical fiber are affected by this temperature effect. However, this can be compensated by a point-to-point thermal compensation or thermal compensation by loop. These compensation methods are based on having a section of the optical fiber unbonded in a small tube or in a loop. Here, the method of thermal compensation by loop was used. The strain dependent on the refractive index and the strain dependent on the thermal expansion of the optical fiber are subtracted from the strain obtained from the bonded part. The results obtained from the measurements proved that the implementation of the optical fibers and the use of the OBR in a real structure over a long monitoring period was successful.

In conclusion, the OBR has given satisfactory monitoring results in a wide range of applications. To verify that it is the right choice for the given application experimental tests as well as finite element analysis are needed. The reviewed research tested samples in a suitable fashion according to fields of application. It is reasonable to find the most prominent life limiting factor for the glass fiber composite repair and perform tests accordingly.

In this thesis, the glass fiber composite bands used for the repair are woven, so one can expect that some voids and resin rich areas will occur around the optical fibers. Consequently, the measurements obtained here may contain more noise than the OBRs potential and it may be reasonable to use the running reference method for strain analysis.

4. CASE STUDY CONFIGURATION

When trying to implement a new monitoring strategy, physical tests are important. Although the OBR is theoretically very promising, there are several practical aspects that provide challenges that need to be dealt with, like handling the fragile optical fiber and introducing noise in the measurements.

In the given application, a composite repair is applied to an offshore riser, mainly operating in the splash zone where air and water temperatures are 25 – 35 °C and 20 – 25 °C respectively. The loads introduced during physical testing should be realistic, and in the given application thermal loads are more likely to limit the lifetime of the repair than mechanical loads. To be a realistic test procedure, yet simple, thermal cycling in water was conducted. Here, the OBR and optical fibers were utilized to detect deformations and possible failures in the repair when subjected to appropriate loads.

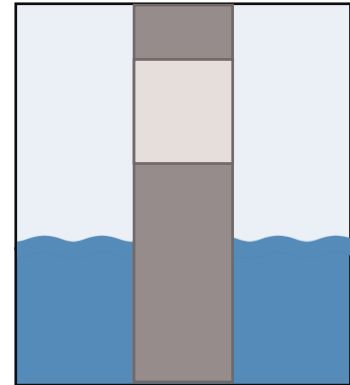


Figure 1 – A repair (light gray) applied on a riser (dark gray) in the splash zone.

Further, the test sample was produced to meet the quality achieved by Kongsberg Ferrotech. Glass fiber composite was applied with tension on a pipe section with the same diameter as a real riser.

Optical fibers were configured to monitor the circumferential behavior of the repair when subjected to thermal cycling loads. By embedding the optical fibers in the repair, i.e. placing them on the interface between the riser and the repair, the strain response originates from the areas of the most interest. This is where debonding is most likely to occur, and defects occurring in this interface are more critical than those occurring in the interface between plies as it is the only load path [22].

4.1 ESTIMATE OF EXPECTATIONS

The value of strain that can be expected by physical testing and finite element analysis was estimated. Since the steel of the riser have a modulus of elasticity much larger than that of the glass fiber composite, in addition to a larger thickness, the expansion of the repair is dominated by the expansion of the riser.

$$\varepsilon = \Delta T \alpha = 70 \cdot 1.17E - 05 = 819 \mu\varepsilon$$

This is a simple estimation that provides verification to the values obtained by testing and numerical analysis. The respective values obtained by FEA and physical testing is elaborated on in Chapter 6.1 and Chapter 7.

5. TESTS

5.1 OBJECTIVE

If any of the relevant failure modes are present, i.e. patch debonding, patch failure or substrate failure, variations in the strain response will be present. In the case of a composite repair in the splash zone, thermal loads are more likely to limit the lifetime of the repair than mechanical loads. To achieve deformations resulting from thermal loads, there were conducted thermal cycling tests.

There was no guarantee that any failure modes would occur during the test. By introducing a predefined failure in a known position, the measurements in this location can be used as a reference to what strain response this failure mode would give. There are several ways to give the test sample such a failure, but a simple and effective method was to place a Teflon film underneath the glass fiber composite. Teflon film will act as a debonding failure and may also act as an initiator, moreover the debonding may continue to grow.

5.2 SYSTEM REQUIREMENTS

The monitoring is performed by using a Luna OBR 4600 delivered by Luna inc, where the full assembly consists of the following components:

- Optical backscatter reflectometer 4600 instrument
- USB cable to connect the OBR instrument to the PC
- Power cord for the OBR instrument
- Laptop or PC with monitor, keyboard, mouse and cables
- Laptop or PC power supply
- Gold reflector
- Software recovery CD-ROM
- Optical fiber connector cleaner
- Optical fiber bulkhead connector cleaners

These components need to be located topside. In addition, primary and secondary coated optical fibers, optical fiber connectors and pig tails are needed. The secondary coated optical fiber will be between the area to be monitored and the OBR; although this part is not measuring the area of interest, it needs to be secured or protected to keep it still. If it moves it may introduce additional noise in the measurements.

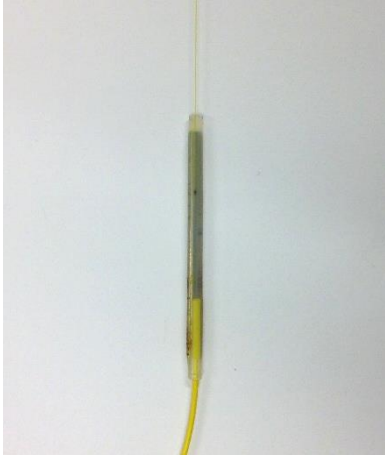


Figure 2 – Primary and secondary optical fiber spliced.

5.3 PREPARATION OF THE OPTICAL FIBER

The optical fiber must be prepared before installation. A section of primary and secondary optical fiber was cut to the desired length, and these two sections were connected or spliced together as shown in Figure 2. These connections may be sensitive and are likely to introduce additional noise, but if connected precisely the connections will not pose as a problem. The optical fiber was prepared by using the equipment shown in Figure 3: wipes, fiber preparation fluid, Fitel S178 Fusion Splicer, scissors, Fitel S325 High Precision Fiber optic cleaver, and a lighter. The primary coated optical fiber was prepared by burning off the coating on a small section at one end. This end section was cleaned by using a wipe and a fiber preparation fluid. A Fitel S325 High Precision Fiber Optic Cleaver was used to give the end of the fiber a clean cut. The primary coated optical fiber was carefully placed in a Fitel S178 Fusion Splicer. Further, the secondary coated optical fiber was prepared by using scissors to remove the coating over a small section at one end, and the remaining fiber was cleaned and cut and placed in the fusion splicer, as described for the primary coated optical fiber. The fusion splicer checks to see if the cut is sufficient and will splice the two ends together. A protector is placed over the spliced area and heated to be secured. The secondary coated optical fiber is to be connected to the OBR, moreover a pigtail needs to be connected to it, i.e. two secondary coated optical fibers are to be connected using the same procedure and equipment.



Figure 3 – Equipment used for the preparation of optical fibers.

5.4 EXPERIMENTAL PLAN

5.4.1 TEST PROCEDURE

The repair system is to be applied in shallow waters where internal, air and water temperature is 60 °C, 25 – 35 °C and 20 – 25 °C respectively. To accelerate deformations in the test sample and reduce the test duration, the temperature difference should be large; the maximum and minimum temperature was chosen to be 90 °C and 5 °C respectively. 90 °C was the maximum working temperature of the composite matrix.

The environmental conditions to affect the performance of the composite repair are water, temperature, UV radiation and chemicals. Here, water and temperature are the only environmental parameters considered. As fresh water has a more severe effect on the composite

repair than saltwater [22], no contamination was introduced other than corrosion from the pipe section itself.

The configuration of the optical fiber was focused on measuring strain in the circumferential direction. There will be more variations in this direction rather than axial, but the configuration of the optical fiber may also be an interesting characteristic to alter in further studies.

TEST SAMPLE

Pipe sections prepared with the coating was provided by Kongsberg Ferrotech, as well as prepreg glass fiber composite. Two test samples were made. When preparing the first test sample the glass fiber was placed over a very short section, making it challenging to apply the glass fiber with an even overlap as well as even tension throughout production. Additionally, some of the optical fibers broke during production. With the acquired experience from the first test sample, the second test sample turned out with presumably good quality.

Four optical fibers were prepared as described in Chapter 5.3. Using several rather than one optical fiber made for easier handling during application, as well as adding redundancy in case any of the optical fibers would break. The optical fiber was placed in the circumferential direction, around the pipe section twice with a smooth turn between each circumferential placement. Fastening the optical fiber with a cyanoacrylate adhesive along its entire length ensure that it stayed in place during the production of glass fiber composite. A section of 28 cm was to be “repaired”, and the optical fiber was placed 1 cm from each edge and configured with 3.25 cm spacing between each fiber, as shown in Figure 4A. This would give a good representation of the entire glass fiber composite repair.

A piece of Teflon film was placed on the surface of the pipe-piece prior to composite production as a predefined failure. At the two outer optical fibers the Teflon film was 2 x 3,5 cm while at the two middle optical fibers the Teflon film was 3,5 x 7 cm.



Figure 4 – A: Configuration of optical fibers and Teflon films. B: Turns were kept smooth. C: Four pieces of Teflon film. Two different sizes were used.

The pipe section was 33 cm long, and the glass fiber composite was applied over a 28 cm segment using the filament winding machine. A setup consisting of an axle and wooden disks

were made to support the pipe section in the filament winding machine, which was used to make the pipe rotate while the actual application of glass fiber composite was executed manually. The composite was applied according to the installation guide in the datasheet enclosed in Appendix A and guidelines provided by Kongsberg Ferrotech's. The first layer was applied by hand without tension, before increasing the tension incrementally. The glass fiber composite was applied in 6 layers with 25 % overlap. At each end of the section where the glass fiber composite was applied, one round of the composite was applied without overlap. To avoid a composite repair with sharp edges every additional layer was 20 mm shorter than the previous, stopping the overlap 10 mm before the edge on each side. The tension was decreased incrementally to finish the application without tension. Each layer was sprayed with water during application to induce the curing process. The final test sample was left to cure in room temperature for a minimum of 72 hours.

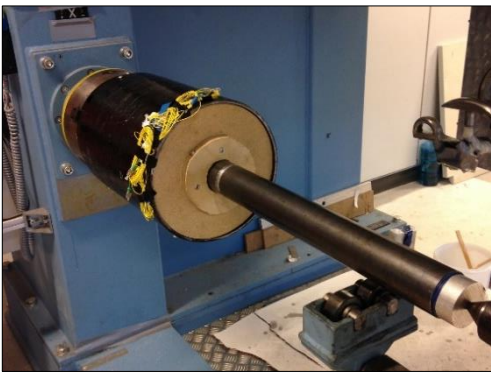


Figure 5 – The test sample assembled in the filament winding machine.

The first test sample provided basis for improvement, so for the second test sample a handle with conical ends made the application easier. Applying the glass fiber composite with tension is essential to the production method to ensure consolidation between the layers and avoids the need of a compressive film. The glass fiber composite had a working time of only 30 minutes, so a simple application method was essential. Since the production was performed manually, there was no measure of how much tension was applied, but the final result appeared with an

overall good quality.

The application of optical fibers is cumbersome and good results require practice. In the first test model, 50 % of the optical fibers broke either during production or de-assembling of the production setup. In the second test sample, a patch of prepreg glass fiber composite was applied where the optical fibers egress the repair. Consequently, all the optical fibers remained intact in the second test sample.

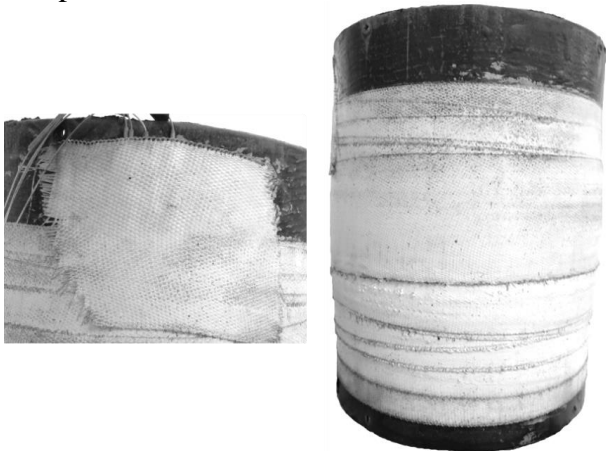


Figure 6 – The glass fiber composite patch protected the optical fibers. The repair possessed good quality. These images were taken after the testing.

TEST SETUP

The thermal cycling was performed using a setup of a pot with an inlet and outlet, cooking plate as well as solid-state relays and Arduino microcontroller for automatic operation. Stabilizing the temperature in the system would serve the purpose of simple interpretation of results.

Initially, the pot was filled with 35 liters of cold water. This was heated, and when the desired temperature of 90 °C was reached, this temperature was kept constant to ensure uniform temperature throughout the system. The total heating process would take 4 hours. To cool the water down to 5 °C, cold water was introduced through the inlet, triggering circulation through the outlet. The cooling process would go on for 4 hours as well. The total time for one cycle was 8 hours. Thermocouples were used to read the temperatures and to tell the Arduino to perform an action. The Arduino logged time and temperature, which was stored on an SD card. The code and setup for the automatic operation is enclosed in Appendix B.

The pot was insulated with Superwool. The set up was secured by a stand and wooden blocks to make sure it would not fall over. A stir rod with a motor was used to ensure uniform temperature in the water. A few square steel beams were placed on the bottom of the pot to raise the test sample, this to ensure uniform temperatures both in the water and the pipe section.

Although different from the actual case of a petroleum production riser, the temperature was kept equal inside and outside the pipe. The objective was to discover failure modes in the glass fiber composite repair, i.e. the focus was on the glass fiber, not the steel. Affecting the temperature in the glass fiber composite from both sides of the pipe section may accelerate variations in the strain response, hence it was argued that was a fair simplification of the tests.

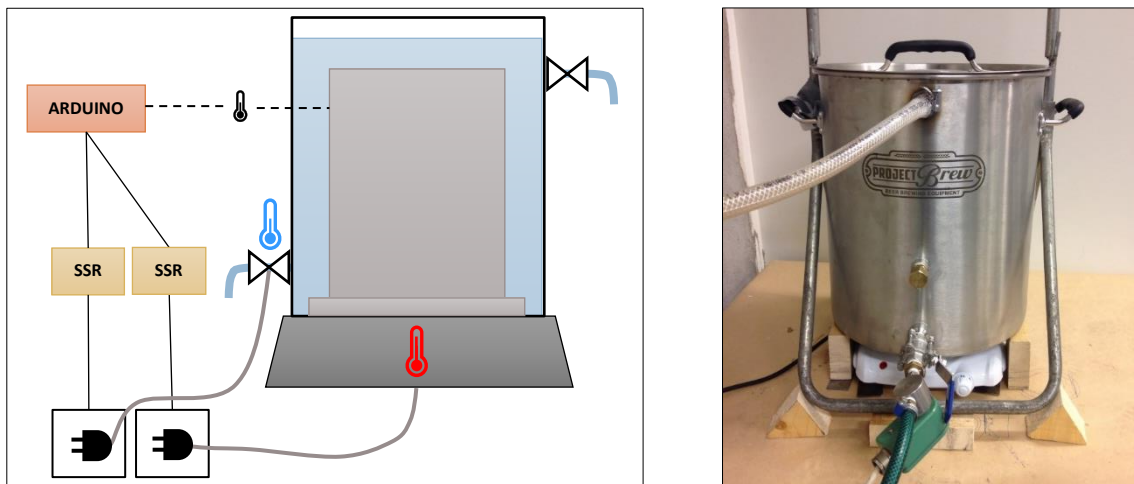


Figure 7 – A: Schematic of the test setup. B: Test setup.

5.5 EXECUTION

Introducing the right amount of water into the system for sufficient cooling was challenging. The valve by the inlet may not have been sufficiently durable, so introducing too much water would also affect the heating. Finding the suitable settings was a process, and it was challenging

to reach the desired temperature of 90 degrees while still reaching a low temperature for the cooling period. By doubling the length of the heating and cooling intervals to give a total cycle period of 16 hours, as well as decreasing the amount of water supplied, a maximum and minimum temperature of 90 and 20 degrees respectively was achieved. Although not ideal, this was the largest temperature difference the test setup would achieve. The tap for the water supply turned out to be surprisingly unpredictable, so the maximum and minimum temperatures were not always constant during each cycle.

The final test parameters were determined on 17.04.19, but the test sample had placed into the test setup on 13.04.19, i.e. introduced to the water and some temperature variations. These temperature variations were ~ 48 hours of low temperatures (15 – 30 degrees) and ~ 48 hours of high temperatures (60 – 90 degrees) respectively. The test was running until 05.05.19.

The measurements were gathered automatically using the measurement software presented by S. Heinze in [34]. Four measurements were taken, one for each optical fiber, every 15 minutes. Each file is ~ 65 Mb and was stored on an external hard drive. The storage capacity was limited, so further on in the test period the measurements were taken every 30 minutes and later every hour.

At an unknown time during the execution of the test the motor for circulation of water stopped working. Consequently, the temperature in the water would not be uniform. The temperature sensor was placed in the upper part of the pot, and as the water was heated from the bottom, the measured temperature would deviate from the actual temperature in the bottom.

Strain data were acquired using the analyzing software presented by S. Heinze in [34]. Most of the data were obtained using one reference file, but the running reference method was also applied. This software made it possible to obtain large amounts of measurements over a long period of time, but it failed to acquire the measurements from optical fiber 2. The measurements did not update from optical fiber 1 to optical fiber 2, so the files obtained from these two optical fibers were equal.

6. FINITE ELEMENT ANALYSIS

To efficiently interpret and analyze the measured data from the tests, a finite element model was developed. The finite element model is a numerical method for predicting the behavior of a structure. This application requires a composite material and a cohesive surface, in addition to the steel riser. Abaqus is known to give accurate results when using such complex materials. Additionally, it supports a wide range of simulation methods. Here, Abaqus 2017 was used.

A similar analysis was performed in the preliminary study. The analysis performed here was improved by modeling the composite repair with more accuracy. Modeling the repair with staircase-like edges is a realistic configuration and will give more accurate results close to the edges. Furthermore, more accurate material properties will be used.

6.1 MODEL

An axisymmetric model was made with the dimensions stated in Table 1 A. The sketch was revolved over 2.5° and based in a cylindrical coordinate system. Models based on symmetry are generally simpler and the analysis require less time.

The part was split into two separate parts to act as the riser and repair respectively. The steel was assigned a section and the common properties of $E = 210E3$ MPa and $\nu = 0.3$, as well as the thermal expansion coefficient $\alpha = 1.17E-05$ [35]. The composite material was defined by a composite layup, where the principal directions was defined by the outer surface and the edge, moreover the 1. direction was given by the hoop direction. The repair was modeled with a staircase structure to mimic the actual repair and to avoid high strain concentrations along the edge. Each step was partitioned and assigned the correct number of composite layers. The composite material was assigned the material properties enclosed in Appendix C, and the dimensions and assumptions are shown in Table 1 A and B.

Table 1 A, B – Properties of the numerical model.

Model Dimensions		Assumptions	
D_{outer}	254 mm	E_3	E_m
t_{steel}	7.4 mm	ν_m	0.4
t_{repair}	1.98 mm	$\nu_{13} = \nu_{23}$	ν_m
l_{steel}	330 mm	$G_{13} = G_{23}$	G_m
l_{repair}	280 mm	α_{33}	1.00E-04

$$G_m = \frac{E_m}{2(1 + \nu_m)} = \frac{3550}{2(1 + 0.4)} = 1268 \text{ MPa}$$

Most of the material properties were, unless otherwise noted, found in the datasheet. Some simple assumptions were made to obtain all the required material properties for an accurate 3D finite element analysis. It was assumed that the glass fiber composite held orthotropic material

properties. However, the shear moduli G_{13} and G_{23} , as well as the Poisson's ratio ν_{13} and ν_{23} was assumed to be equal to the respective properties of the polyurethane matrix as given in Table 1B. The assumptions made for these out-of-plane properties are obviously simple and represents the lower bound values for the stiffness. However, the structural behavior is presumed to be dominated by the in-plane properties anyways. The value of the thermal expansion coefficient α_{33} was assumed to be approximately double the values of α_{11} and α_{22} .

Although these are rough assumptions, it was argued that the strain is dominated by the material properties of the steel riser. Furthermore, variations in the material properties for the glass fiber composite will not greatly affect the strain response.

The model of the riser and repair is shown in Figure 8. Two displacement/rotation boundary conditions were defined, one to support the bottom surface in the z-direction of the cylindrical coordinate system, and one to support the side surface in the θ -direction of the cylindrical coordinate system. The boundary conditions are shown in Figure 9A.

The riser was assigned a structured mesh with size 6 mm, while the repair was assigned a sweep mesh, see Figure 9B. The repair was modeled with the thickness of 6 layers, i.e. 1.98 mm, and each layer in the staircase configuration was modeled with the thickness corresponding to the thickness of the given point, i.e. 0.33 mm at the smallest. The size of the mesh was assigned to be 1.98 mm to most of the repair. The two bottom layers closest to the edge of the repair was assigned a smaller mesh size using bias, moreover the size of the mesh would gradually increase from 0.33 to 0.99 mm as the distance from the edge increased.

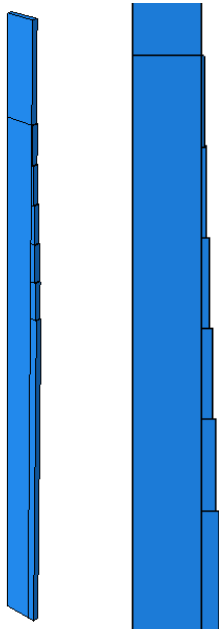


Figure 8 – Model of riser and repair.

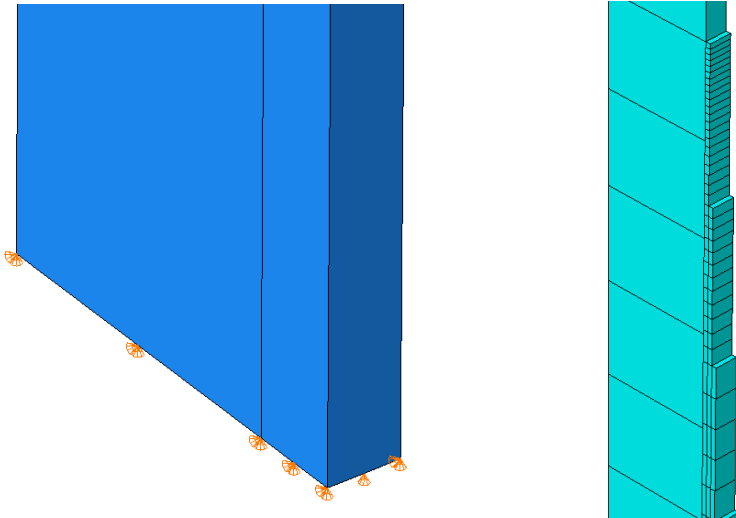


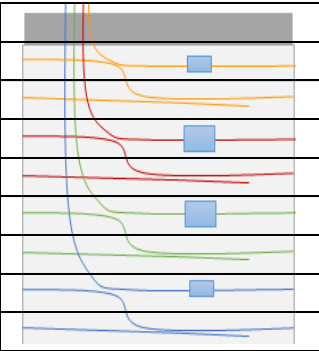



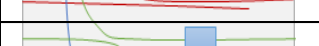

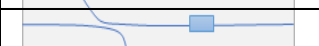


Figure 9 – A: Two boundary conditions were defined. B: Mesh of the model.

To act as the corrosive resistive coating between the riser and the repair, a cohesive surface was defined rather than a cohesive element. This is a simplified way to model cohesive connections, assuming the thickness is of negligible size. Additionally, it supports failure in traction-separation. Neglecting the thickness and the mass of the coating was a fair assumption as its actual thickness is 500 μm , moreover significantly less than the other components. The cohesive surface was built on an interaction contact, which was defined by contact pairs. The contact pair was defined as the surface between the two parts. The traction-separation behavior was applied to the slave nodes initially in contact.

To construct the analysis, an additional step to the initial needed to be defined. The default step, static general, was defined. Thermal strain was triggered by defining a predefining field with a temperature change of 70 $^{\circ}\text{C}$.

The hoop strain detected from the physical tests can be expected to have a strain value as enclosed in Table 2, which corresponds well with the value found by the analytical estimate. The strain distribution for the top and bottom surface of the repair is shown in Figure 10, which gives an idea of the comprehensive response of the repair rather than the detailed display of Table 2. From Table 2 it is clear that the strain response is the highest along the edges of the repair.

Table 2 – Strain values obtained from FEA corresponding to the positions of the optical fibers. The notation a and b correspond to the first and second circumferential placement of the optical fiber respectively.

Position	Microstrain	
OF1, a	850.3	
OF1, b	824.7	
OF2, a	818.2	
OF2, b	818.4	
OF3, a	818.4	
OF3, b	818.2	
OF4, a	824.7	
OF4, b	850.3	

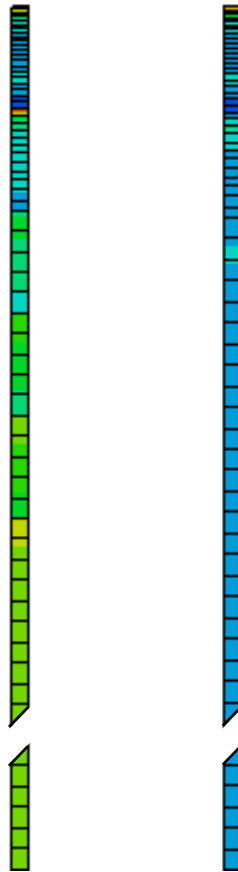
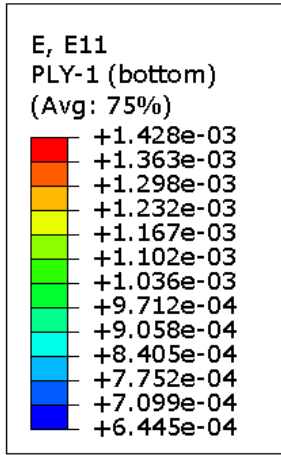


Figure 10 – Strain distribution for the top surface (left) and bottom surface (right).

7. RESULTS AND DISCUSSION

Prior to the application of the repair, reference points in the optical fiber were defined. These points were located as shown in Figure 11. A small point load was applied to the reference points while performing a scan with the OBR. The location of reference points and Teflon films were found and are presented in Table 3.

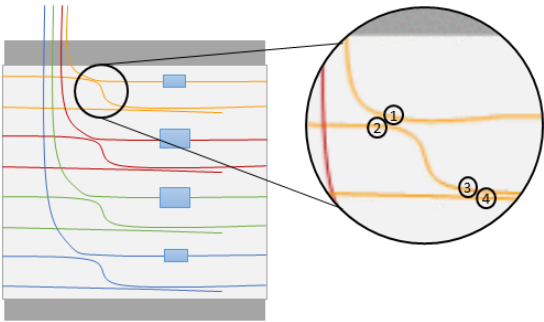


Figure 11 – Configuration of optical fibers and location of reference points.

Table 3 – Reference points and their corresponding location on the optical fiber.

Optical fiber	Reference point	Location [m]
OF1	1	16.30
	2	17.12
	3	17.25
	4	18.45
	Teflon	16.44 – 16.475

Optical fiber	Reference point	Location [m]
OF3	1	17.00
	2	17.88
	3	17.94
	4	18.86
	Teflon	17.12 - 17.19

Optical fiber	Reference point	Location [m]
OF2	1	17.80
	2	18.64
	3	18.70
	4	19.40
	Teflon	17.90 - 17.97

Optical fiber	Reference point	Location [m]
OF4	1	17.36
	2	18.18
	3	18.30
	4	19.20
	Teflon	17.49 - 17.525

The temperature cycles that the test sample was subjected to is revealed in Figure 12. Clearly, the temperature amplitude was irregular. The area marked in red was not considered as part of the main test duration, meaning that only some strain data was collected from this time period. The optimal test parameters were found on 17.04.19, i.e. $t = 330\,000$ s, and is from here on referred to as $t = 0$. Although the test sample had been exposed to temperature cycles prior to this time, the test parameters after this point were as expected. What was the most interesting to study was the development of the areas around the predefined failures, and if there were some strain development that needed more explanation, strain data could be obtained from the measurements in the marked area. This part of the test is from now on referred to as trial cycles. Further, the measurements originating from the temperature cycles after 1 300 000 s in Figure 12 were affected by computer issues and are therefore limited.

The strain data was acquired using software made to analyze the OBR files automatically [34]. Most of the strain data was calculated using the first measurement file obtained on 17.04.19 as reference. Some strain data suffered from noise. The strain data with the most prominent noise effects, which were the 92 first measurements on OF3, were re-calculated using both the running reference method and different parameters of strain calculation to reduce the noise effects.

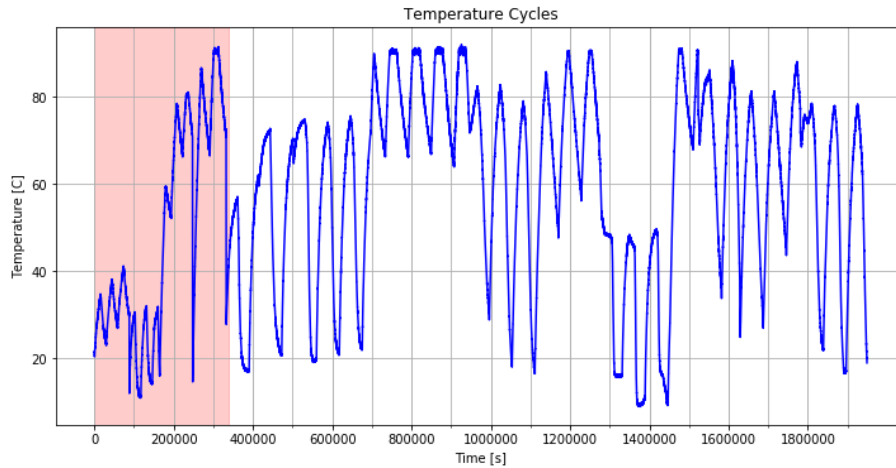


Figure 12 – Temperature cycles. The area marked in red was not considered part of the main test execution and was in some cases disregarded.

7.1 STRAIN IN RELATION TO TEMPERATURE

As seen in Figure 13, there is a clear correlation between temperature and strain. When heated, the glass fiber composite and hence the optical fiber expands. As the test specimen had been subjected to the trial cycles, the predefined failure can already be observed.

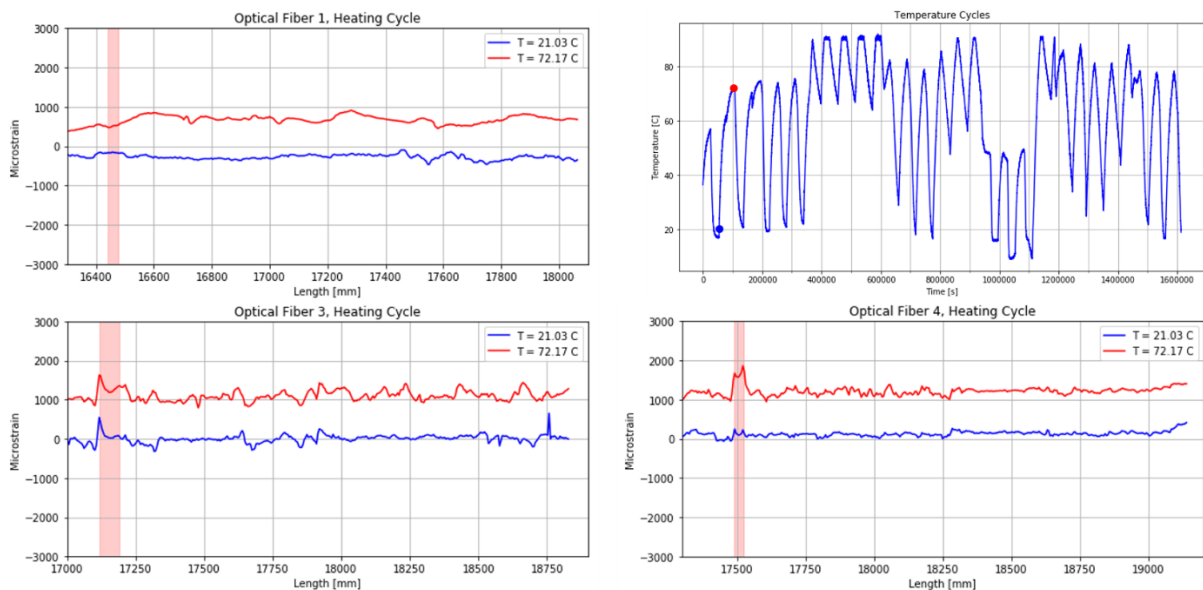


Figure 13 – A, C and D: Heating cycles gathered from measurement 66 (blue) and 125 (red). B: Temperature cycles throughout the test duration. Measurement 66 and 125 are marked with a blue and red dot respectively.

At some time, the device used for circulation of water stopped working, resulting in a non-uniform temperature distribution. Figure 14 reveals that there was a noticeable lag between the temperature and strain measurements. The temperature was measured in the upper part of the pot and heated from the bottom, so this trend would be the most prominent in the upper part of the pot. For optical fiber 1, which was located in the upper part of the pot, the measured temperature lags the strain response. For optical fiber 3 and 4, however, this lag is only apparent for cooling. The average strain value found from optical fiber 1 is low compared to optical fiber

3 and 4. The actual temperature is most likely higher than the measured temperature in the bottom of the pot, causing more severe deformations.

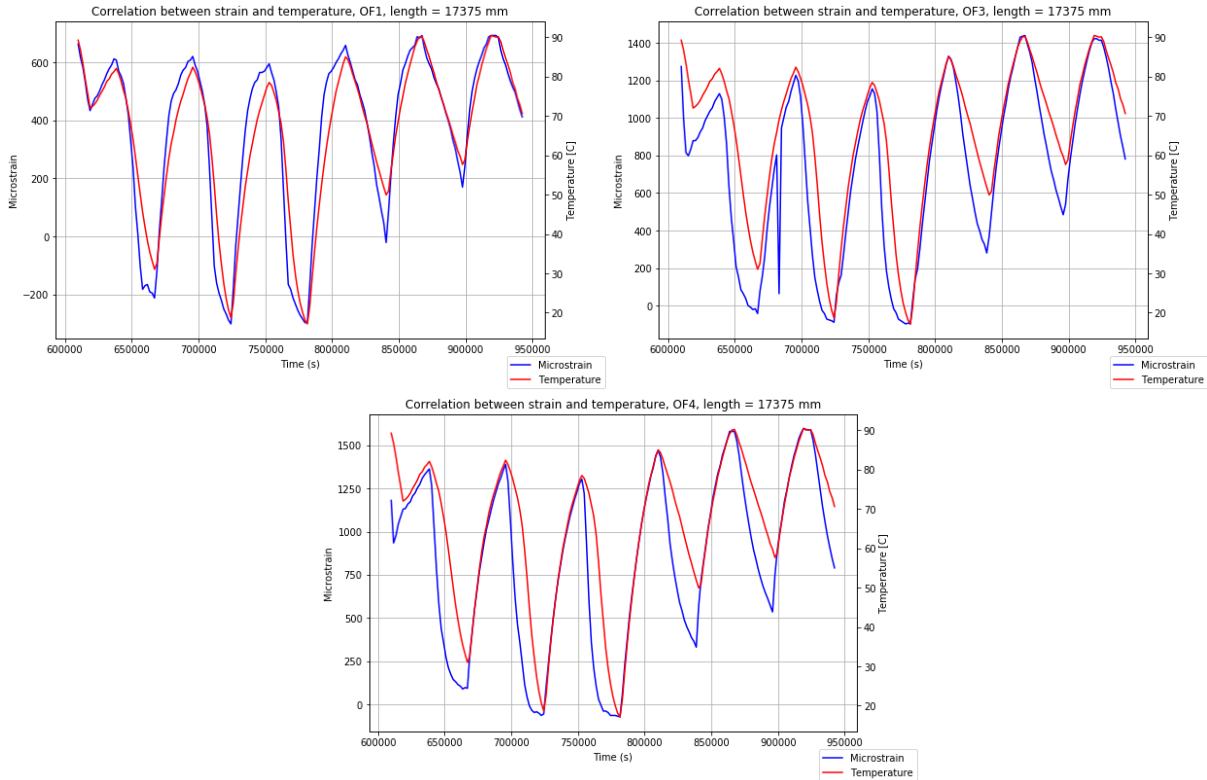


Figure 14 – There was an obvious lag between temperature and strain.

7.2 DEBONDING

The predefined failures could clearly be recognized in the strain data obtained from optical fiber 3 and 4, as seen in Figure 15, with an indication of what strain response a debonding failure gives. As the temperature increases, the difference in strain value of the debonding failure and the area around increases. As the temperature decreases, on the other hand, this debonding characteristic and the difference in this strain value fades. Optical fiber 1 showed no such characteristic. The full development of the areas around the predefined failures of optical fiber 1, 3 and 4 are presented in films enclosed in Appendix E, F, G and H, where Appendix F includes the strain development detected by optical fiber 3 during the trial cycles.

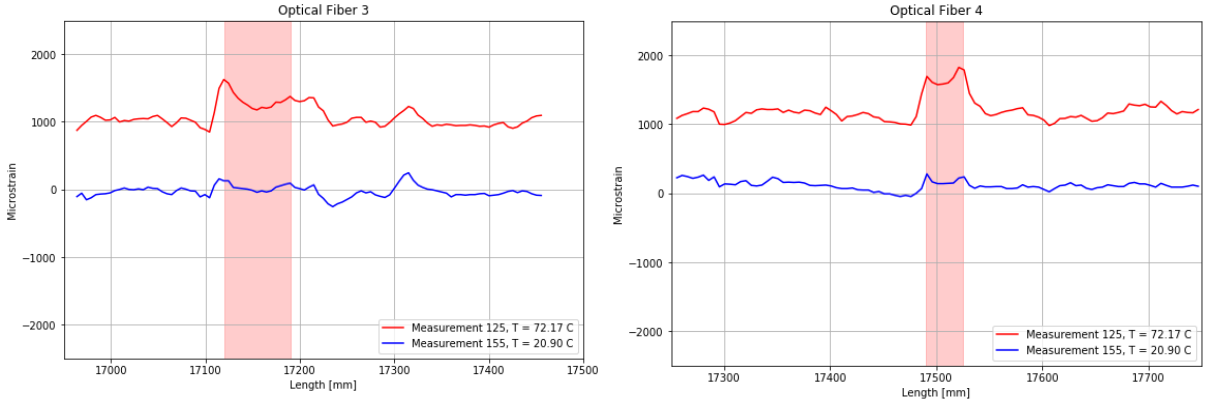


Figure 15 – The debonding characteristic changes according to the temperature.

During the main test period, the debonding failures is observed not to grow. Growth of the debonding is recognized by a larger distance between the two peaks, which cannot be found in Figure 16. However, on optical fiber 3, the debonding failure appears larger than the size of the Teflon film, which may suggest that the debonding failure developed during the trial cycles. As shown in Appendix F the predefined failure could be seen after measurement 147, and the elongation of the debonding characteristic can be seen after measurement 161 of the trial cycles. This elongation is not necessarily growth but may be inconsistent adhesion between the glass fiber composite and the steel riser around the predefined failure that occurred in the production process. Throughout the test execution, the debonding characteristic becomes more prominent but does not seem to grow.

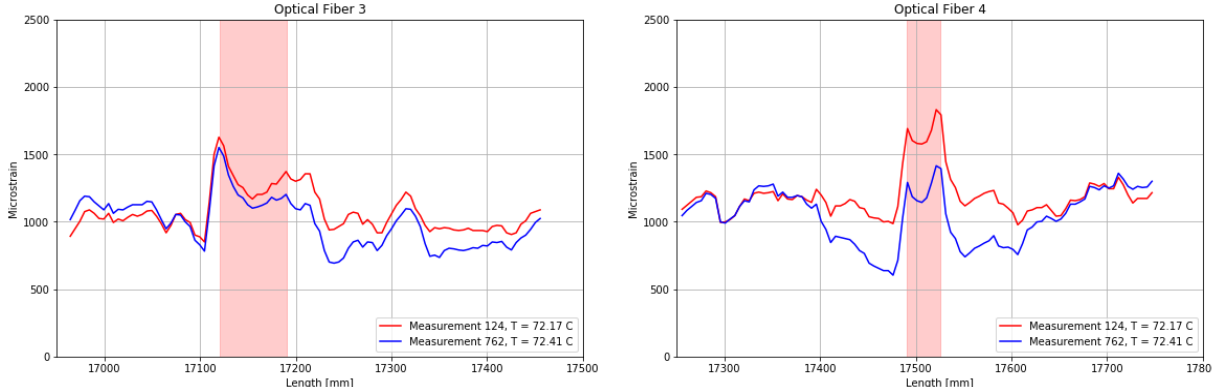


Figure 16 – Development of the debonding failures detected by OF3 and OF4.

On the basis of Figure 16 and Appendix G, no conclusion of an increasing peak strain in the debonding failure can be drawn. Although the temperature is approximately the same, measurement 124 has a higher peak strain than measurement 762. The peak strain is more dependent on the temperature than the total cycle exposure time.

In the strain data obtained from optical fiber 3, two peaks appear at the location ~17300 and ~17400 mm of the length of the optical fiber, as shown in Figure 17. The former is prominent at high and low temperatures, while the latter is only prominent at lower temperatures. There are several possibilities of why such peaks appear in the measurements. When the optical fiber is applied to the surface of the pipe section it may contain small bends. An increased temperature causes the optical fiber to expand and this bend will fade, while when the

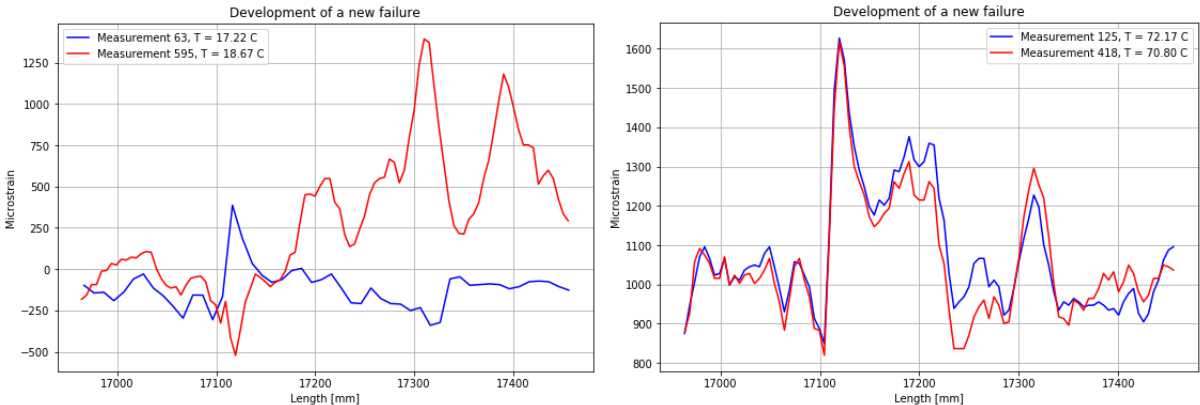


Figure 17 – Development of a new failure.

temperature decreases the optical fiber can buckle which will show up as a peak in the measurements. When a peak is more prominent at lower temperatures, the optical fiber buckling is more likely than failures in the glass fiber composite. It is possible that the peak at ~17300 mm, which is present at high and low temperatures, is a delamination failure similar to what was found by Díaz-Maroto et al. in [30]. However, irregularities on the riser surface will also cause peaks in the strain response.

7.3 STRAIN DATA FROM TEST AND FEA

A comparison between the strain data detected by OBR monitoring and FEA are presented in Table 4 and 5. The strain data detected by optical fiber 1 corresponded fairly well with the strain found from the FEA and the analytical estimation in Chapter 5.1. The difference between these values are within the range of what one can expect when performing such tests. As stated in 5.5, the OBR software did not successfully measure the deformations detected by optical fiber 2, so these values are not included. The strain detected by optical fiber 3 and 4 deviates from the values obtained by FEA. A deviation of around 200 % is severe, and the strain distribution from the test was not symmetric as expected.

Table 4 – Strain from FEA and measurement 705, $T = 90.02$ °C.

	Reference point	FEA, $\mu\epsilon$	Test, $\mu\epsilon$	Ratio
OF1	1	850.3	548.0	74
	2	850.3	828.3	112
	3	824.7	1040.8	126
	4	824.7	802.8	97

OF2	1	818.2	-	-
	2	818.2	-	-
	3	818.4	-	-
	4	818.4	-	-

OF3	1	818.4	1486.7	182
	2	818.4	1631.1	199
	3	818.2	1809.6	221
	4	818.2	1329.5	163

OF4	1	824.7	1609.9	195
	2	824.7	1631.0	198
	3	850.3	1673.6	225
	4	850.3	1665.1	224

Table 5 – Strain from FEA and measurement 401, $T = 89.13$ °C

	Reference point	FEA, $\mu\epsilon$	Test, $\mu\epsilon$	Ratio
OF1	1	850.3	522.3	70
	2	850.3	794.3	107
	3	824.7	1057.7	128
	4	824.7	938.6	114

OF2	1	818.2	-	-
	2	818.2	-	-
	3	818.4	-	-
	4	818.4	-	-

OF3	1	818.4	1350.7	165
	2	818.4	1563.2	191
	3	818.2	1656.6	203
	4	818.2	1588.6	194

OF4	1	824.7	1558.8	189
	2	824.7	1631.1	198
	3	850.3	1550.5	209
	4	850.3	1694.7	228

Because of the non-uniform temperature, the temperatures at the location of optical fiber 3 and 4 have most likely been higher than 90 degrees, which is the maximum working temperature for the glass fiber composite. Consequently, the deformations that occurred here are more severe. The fact that the Teflon film on optical fiber 1 cannot be seen in the strain data supports

this statement. If the temperature was within the working temperature of the class fiber composite throughout the test duration, it is clearly not guaranteed that the predefined failures may not have been detected.

The peak strain from Figure 15 and Figure 16 is in the range of 1500 – 2000 $\mu\epsilon$ at high temperatures. This value deviates significantly from the findings in FEA, hence, this could be values to expect in the case of debonding failures.

7.4 VISUAL INSPECTION

Figure 18 shows the repair after the execution of the test. The surface of the repair appeared unaffected by the temperature variations, and the documented debonding was not discovered by visual inspection. Some lumps of polyurethane were progressing along an edge of the glass fiber composite band. The glass fiber composite may not have been saturated enough with water during the application of the repair or the cure time was not satisfactory. Clearly, corrosion occurred where the corrosion resistive coating was not applied, i.e. in holes and along the top edge, as revealed in Figure 18.

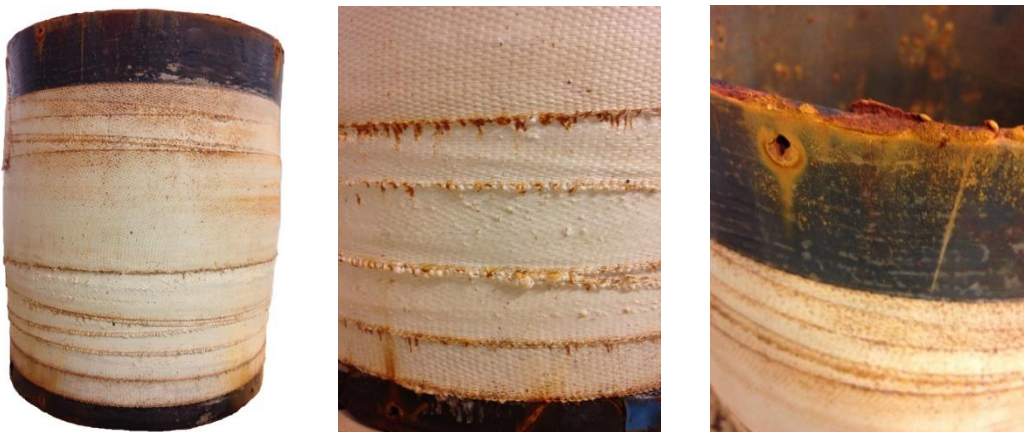


Figure 18 – Appearance of the repair after the execution of the test.

7.5 NOISE

The measurements that contained the most noise was recalculated using the running reference method. However, these running reference measurements contained too much noise for this method to give satisfactory results. This method uses the latter measurement as reference and adds up the strain values from all measurement files to find the final strain value. It interpolates between measurement points, and therefore requires that most of the measurement points do not contain noise. This noise will in that case be added to the strain values from the next file, and one will finally end up with more noise. Approximately 90% of the noise is automatically detected [29], but can be improved by manual interpolation.

Re-calculating the measurements with a larger gauge length and sensor spacing decreased the noise content significantly. In Figure 19, two strain curves are obtained from the same

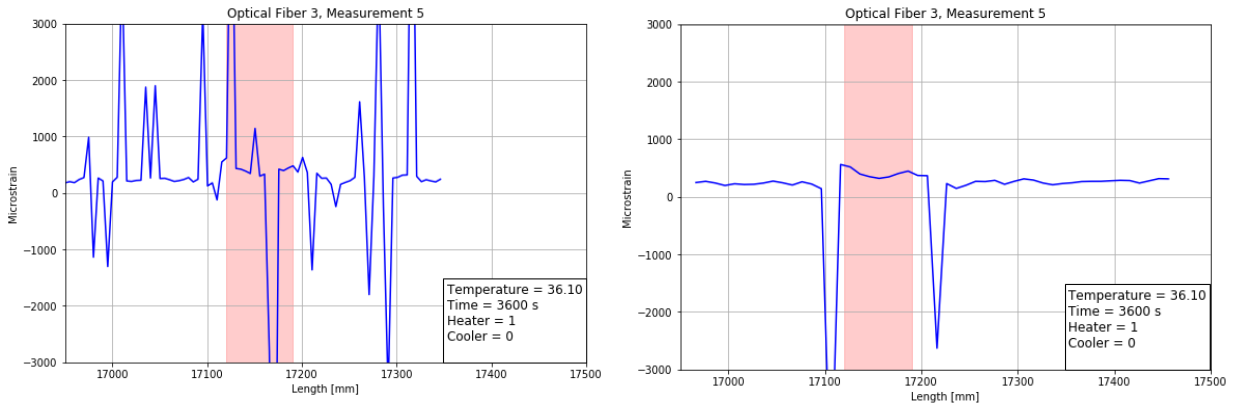


Figure 19 – Strain curves from measurement 5. The strain curve on the left is shorter because a different mid-point was used for the calculation.

measurement, i.e. the same OBR file. The strain curve containing the most noise was calculated using a gauge length of 5 mm and a sensor spacing of 5 mm, which was the same that was used for most of the other strain calculations. Due to the large noise content, the strain data was recalculated using a gauge length of 10 mm and a sensor spacing of 10 mm, resulting in a significant decrease of noise. Here, there are only two points that are considered noise, which can be removed using simple interpolation.

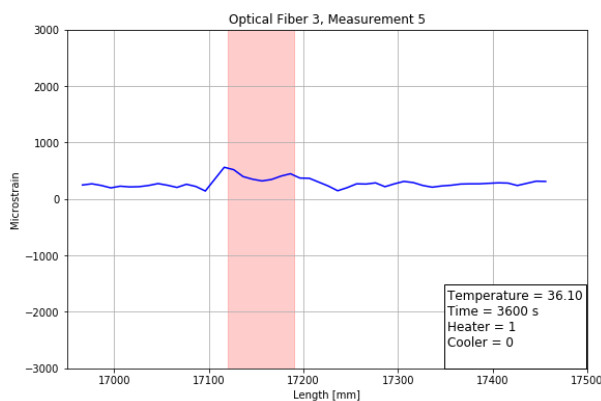


Figure 20 – Strain curve from measurement 5 without noise.

several other reasons for noise, like disturbances to the secondary coated optical fibers, faulty splices and bad connections, which are reasons just as likely to have caused this noise. Further, the points of intersection between the optical fibers are a source of noise but will not affect the entire measurement such as in Figure 19. Most of the measurements turned out with good quality without the use of noise reduction methods, and there was no correlation between noise and temperature.

7.6 EVALUATING QUALITY OF RESULTS

In the conducted research, there are several elements that contribute to margin of error. First, the average strain is dominated by the coefficient of thermal expansion for steel. This value depends on the composition of the material and will bring uncertainties when assumptions are made. Further, the coefficient of thermal expansion for the glass fiber composite, α_{33} , was not

stated in the datasheet and was assumed to be 1.00E-04. Using different values for the coefficient of thermal expansion will give large effects in FEA. The other material properties that were assumed will also bring uncertainties, but not to the same extent as the coefficient of thermal expansion. The assumptions made to the numerical model seemed to be good estimates, as the values obtained here corresponded well with the simple analytical estimation as well as the strain values detected by optical fiber 1.

The numerical model appears to be a good representation for the actual test sample and its staircase-like structure along the edges did not give any noticeable high strain concentrations. However, applying the glass fiber composite by hand will obviously give variations in tension and overlap, and will not be identical to the numerical model.

Furthermore, the quality of the repair will clearly not uphold the quality achieved by a machine. If the repair had been applied with a machine by Kongsberg Ferrotech's methods, production parameters such as tension and overlap would be more consistent. Applying the glass fiber composite with tension ensures consolidation between the layers of the laminate, moreover inconsistent tension may cause areas weaker than the repair's average integrity. From Figure 13 A, C and D, the strain response is clearly smoother in some areas than others. If the repair had been prepared by a machine, one could expect the strain response to be smoother throughout the monitored area, especially considering the strain response originating from optical fiber 3. As the predefined failures were clearly detected, the repair is sensitive to irregularities on the riser surface.

The OBR is a suitable monitoring technique for early detection of damage and monitoring failures to verify that the riser's integrity is satisfactory. The predefined failures were detected, and no growth of these failures were recorded. To conclude on the damages' influence on the structural integrity, more tests with longer durations are needed.

As previously stated, the device used for heat circulation stopped working and led to inaccurate temperature measurements and a non-uniform temperature distribution in the water. The temperature seemed to be higher in the bottom part of the pot. Consequently, optical fiber 3 and 4 was more affected by the temperature variations and the predefined failures were clearly visualized, while no such failure was detected by optical fiber 1. The non-uniform temperature also caused the temperature measurement to deviate from its corresponding strain measurement. Further, the electrical input valve and the water tap were unpredictable and gave irregular water intake, which caused uneven temperature changes and may also have affected the water level.

The configuration of the optical fibers provided strain results from the entire interface between riser and repair. This gave large amounts of measurement data. Here, mainly the areas around the predefined failures were analyzed rather than data acquired from the entire length of the optical fiber, as a limitation to the amount of data to analyze.

OBR monitoring requires large amounts of storage capacity, and an USB hard drive was used. When this was full, however, a few measurements were acquired to a USB flash drive. The

flash drive required more time to save each file, consequently, the automatic measurement software did not work properly. Similar to what happened for optical fiber 2, not all measurements originated from the correct optical fiber. When conducting the strain analysis, the strain data acquired from these files were nothing but noise. Further, computer trouble affected the data collected after measurement 717. The computer went to sleep mode and the automatic OBR program stopped, resulting in a limited number of measurement files from the last duration of the test execution.

When using the OBR for strain monitoring, .obr files being the full measurement file and .txt files being the strain data cannot be acquired simultaneously. Moreover, the test was stopped to develop the strain data, and with the large amount of measurement files, this was a time-consuming process. This was a limiting factor to the extent and duration of the test.

7.7 CONCLUSION

The OBR monitoring gave useful results and provided helpful experience with the use of OBR for strain monitoring over a fairly long time period. None of the optical fibers broke, which proves the OBR to be a durable monitoring technique.

The predefined failures were referred to as debonding failures because this area had no cohesion between the glass fiber composite and the riser. The debonding that was detected as a result of the predefined failures can similarly occur because of surface irregularities or inconsistent coating application. These predefined failures did not occur because of the thermal cycling, but the lamination process, as they were introduced during manufacturing. Furthermore, the repair is sensitive to inaccuracies during production.

One of the main issues with a debonding failure is growth, the larger the debonding failure is the weaker the structure will be. Neither growth nor increase in peak strain was detected in the present study. Moreover, no conclusion can be drawn about the effects on the structural integrity of the repair due to the debonding failure. In order to conclude on the repair's long-term response to thermal cycling more tests with a longer test duration is needed. Appendix F shows the strain response detected by optical fiber 3 during the trial cycles, and the predefined failure was visible after measurement 147. The debonding characteristic became clearer after this point but did not grow. The test sample had been subjected to 38 temperature cycles in total (i.e. trial and main cycles), although with different amplitudes.

8. CONCLUSION

The presented research demonstrates that the optical backscatter reflectometer (OBR) is well suited for strain monitoring in applications of composite repairs on risers subjected to thermal cycling. Optical fibers were embedded in the glass fiber composite to monitor the interface between riser and repair and were configured to give the strain response from the entire repair rather than a few single points. In the egress region the optical fibers are vulnerable to breakage but were successfully protected by a small patch of glass fiber composite. The strain data possessed adequate quality with high resolution.

The numerical model was a good representation of the physical test sample. However, the strain values found in FEA will obviously deviate from the actual strain values when making assumptions to material properties and performing the repair production by hand.

Early detection of damage is essential to verifying that the structural integrity is intact. The repair process performed here was most likely satisfactory because the detected predefined failures did not grow. OBR monitoring also detected other variations in strain, which may have been caused by buckling of the optical fiber, irregularities on the riser surface or delamination of the repair.

9. FURTHER WORK

In the presented study, only one test sample was properly tested. The collection of strain data from the measurements was time consuming, so the extent and duration of the test was limited. To create statistics, more tests with longer durations are needed. However, consistency in production by an automated repair application may provide clear correlations between strain response and production quality. It is of interest to perform tests with shorter cycles to reduce the required time, which can be achieved by using more powerful heating and cooling devices. The temperature difference was intended to be as large as possible, but with the chosen test setup the lowest temperature achieved was just below 20 °C. Further, subjecting the sample to temperature shocks may be of interest. This is more realistic than keeping heating and cooling cycles to the same duration and can also decrease the overall duration required to achieve long term developments.

The results showed peaks in the strain response, but whether this was in fact delamination or e.g. irregularities on the riser surface was uncertain. Other monitoring techniques like C-scan can be utilized as a verification of patch failure. In further tests, a crack can be implemented on the riser surface in addition to Teflon films to distinguish between failure modes.

The optical fibers were configured to monitor the behavior of the repair in the hoop direction. For repairs of a larger scale, the deformations are the largest in the axial direction, and it may be of interest to configure the optical fibers to monitor this direction as well.

To implement the OBR in real case scenarios, several aspects need accounting for. How to include the application of optical fibers in the current repair production needs to be investigated. Further, the secondary coated optical fibers need to be secured to avoid introducing unnecessary noise or breaking of optical fibers.

10. REFERENCES

1. Lamvik, K.S., *Development of Methods for Monitoring Composite Repair on Risers*. 2018, Department of Mechanical and Industrial Engineering: NTNU.
2. DNV, *DNVGL-OS-C201 Structural design of offshore units - WSD method*. 2015.
3. Lozev, M., R. Smith, and B. Grimmett. *Evaluation of methods for detecting and monitoring of corrosion damage in risers*. in *ASME 2003 22nd International Conference on Offshore Mechanics and Arctic Engineering*. 2003. American Society of Mechanical Engineers.
4. Chen, J., Y. Huang, and X. Dong, *Study on the splash zone corrosion protection of carbon steel by sacrificial anode*. *International Journal of Electrochemical Science*, 2012. **7**(5): p. 4114-4120.
5. Oil & Gas Journal, *Rubber coating protects platform riser*. *Oil & Gas Journal*, 1998. **96**(49): p. 66.
6. Sykes, D.J., *Metallurgical Failures in Oil and Gas Pipelines*. 2012, Asia Offshore Energy Conference.
7. Guo, B., S. Song, A. Ghalambor, and T.R. Lin, *An Introduction to Condition-Based Maintenance*, in *Offshore Pipelines*. 2014. p. 257-297.
8. Singh, R., *Chapter One - Need for the Study of Corrosion*, in *Corrosion Control for Offshore Structures*, R. Singh, Editor. 2014, Gulf Professional Publishing: Boston. p. 3-6.
9. Singh, R., *Chapter Two - Corrosion Principles and Types of Corrosion*, in *Corrosion Control for Offshore Structures*, R. Singh, Editor. 2014, Gulf Professional Publishing: Boston. p. 7-40.
10. Bardal, E., *Korrosjon og korrosjonsvern*. 1985, Trondheim: Tapir.
11. UNSW School of Materials Science and Engineering. *Types of Corrosion: 5. Crevice Corrosion*. 2013 7/11/18]; Available from: <http://www.materials.unsw.edu.au/tutorials/online-tutorials/5-crevice-corrosion>.
12. Nimmo, B. and G. Hinds, *Beginners guide to corrosion*. NPL, Teddington, 2003.
13. Lim, K.S., S.N.A. Azraai, N.M. Noor, and N. Yahaya, *An Overview of Corroded Pipe Repair Techniques Using Composite Materials*. *International Journal of Materials and Metallurgical Engineering*, 2016. **10**(1).
14. Duong, C.N., *Composite repair: theory and design*, C.H. Wang, Editor. 2007, Elsevier.
15. Echtermeyer, A.T., D. McGeorge, J.H.L. Grave, and J. Weitzenböck, *Bonded patch repairs for metallic structures – A new recommended practice*. *Journal of Reinforced Plastics and Composites*, 2013. **33**(6): p. 579-585.
16. Wan, B., *Using fiber-reinforced polymer (FRP) composites in bridge construction and monitoring their performance: an overview*, in *Advanced Composites in Bridge Construction and Repair*. 2014. p. 3-29.
17. Ma, W.F., J.H. Luo, and K. Cai, *Discussion about Application of Composite Repair Technique in Pipeline Engineering*. *Advanced Materials Research*, 2011. **311-313**: p. 185-188.
18. DNV, *DNV-RP-C301 - Design, Fabrication, Operation and Qualification of Bonded Repair of Steel Structures*. 2012.
19. Kongsberg Ferrotech. *Oktapous*. 2018 14.11.18]; Available from: <https://www.kferrotech.no/oktapous/about-oktapous/>.
20. Figliola, R.S., *Theory and design for mechanical measurements*. Sixth edition. ed, ed. D.E. Beasley. 2015, Hoboken: John Wiley & Sons.

21. Luna inc, *Distributed Fiber Optic Strain Sensing: Applications in Composites Test and Measurement*. 2013.
22. DNV, *DNV-OS-C501 - Composite Components*. 2013.
23. Palmieri, L., *Distributed Optical Fiber Sensing Based on Rayleigh Scattering*. The Open Optics Journal, 2013. **7**(1): p. 104-127.
24. Luna inc, *Optical Backscatter Reflectometry (OBR) - Overview and Applications*. 2018.
25. Grave, J.H.L., M.L. Håheim, and A. Echtermeyer, *Measuring changing strain fields in composites with Distributed Fiber-Optic Sensing using the optical backscatter reflectometer*. Composites Part B: Engineering, 2015. **74**: p. 138-146.
26. Grave, J.H.L., M.L. Håheim, and A. Echtermeyer, *Evaluation of the Strain Field in a Composite - Metal Ashesive Joint with an Optical Backscatter Reflectometer*. 2012, ECCM.
27. Saeter, E., K. Lasn, F. Nony, and A.T. Echtermeyer, *Embedded optical fibres for monitoring pressurization and impact of filament wound cylinders*. Composite Structures, 2019. **210**: p. 608-617.
28. Lasn, K., E. Sæter, and A. Echtermeyer. *Sensing of Structural Damage with OBR Based Fibre-Optic Networks*. 2018. STO-Meeting Proceedings Paper.
29. Heinze, S. and A. Echtermeyer, *A Running Reference Analysis Method to Greatly Improve Optical Backscatter Reflectometry Strain Data from the Inside of Hardening and Shrinking Materials*. Applied Sciences, 2018. **8**(7).
30. Díaz-Maroto, P., A. Fernández López, B. Larrañaga, and J.A. Güemes Gordo, *Free-edge delamination location and growth monitoring with an embedded distributed fiber optic network*. 2016.
31. Bernasconi, A., M. Carboni, L. Comolli, R. Galeazzi, A. Gianneo, and M. Kharshiduzzaman, *Fatigue Crack Growth Monitoring in Composite Bonded Lap Joints by a Distributed Fibre Optic Sensing System and Comparison with Ultrasonic Testing*. The Journal of Adhesion, 2015. **92**(7-9): p. 739-757.
32. Wong, L., N. Chowdhury, J. Wang, W.K. Chiu, and J. Kodikara, *Fatigue Damage Monitoring of a Composite Step Lap Joint Using Distributed Optical Fibre Sensors*. Materials (Basel), 2016. **9**(5).
33. Barrias, A., G. Rodriguez, J.R. Casas, and S. Villalba, *Application of distributed optical fiber sensors for the health monitoring of two real structures in Barcelona*. Structure and Infrastructure Engineering, 2018. **14**(7): p. 967-985.
34. Heinze, S. *Software Used to Obtain Data*. Available from: <https://github.com/SorenHeinze/OBR-Running-Reference-Method-Software>.
35. ToolBox, E. *Temperature Expansion Coefficients of Piping Materials*. 2003 [21.05.19]; Available from: https://www.engineeringtoolbox.com/pipes-temperature-expansion-coefficients-d_48.html.